applied sciences

MDPI

Article

The Modification Mechanism of Nano-Liquids on Streamer Morphology and Breakdown Strength under Microsecond Pulse

Diangeng Li [1,2], Zicheng Zhang [1,2,*], Shifei Liu [1,2] and Song Li [1,2]

[1] College of Advanced Interdisciplinary Studies, National University of Defense Technology, Changsha 410073, China; diangengli18@nudt.edu.cn (D.L.); liushifei16@nudt.edu.cn (S.L.); song_lisong111@nudt.edu.cn (S.L.)

[2] State key Laboratory of Pulsed Power Laser Technology, Changsha 410073, China

* Correspondence: zczhang@nudt.edu.cn

Received: 22 September 2020; Accepted: 15 October 2020; Published: 21 October 2020

check for updates

Abstract: In liquid mediums, whether the breakdown strength can be greatly improved after introducing the nano-particles has been widely investigated, however, there has been no scientific consensus on the modification mechanism of this anomalous phenomenon. In this paper, we first experimentally measured the streamer morphology and breakdown strength in pure transformer oil, TiO_2 nano-liquids and Al_2O_3 nano-liquids under microsecond pulse. The results demonstrated that there are significant differences in streamer morphology between pure transformer oil and nano-liquids, as the streamers in pure transformer oil exhibit thick bush-like qualities, while in nano-liquids they exhibit tree-like qualities. Moreover, the breakdown voltage results show that the breakdown strength of transformer oil is improved after nano-modification, and the TiO_2 nano-liquids and Al_2O_3 nano-liquids have nearly the same optimal volume fraction. The results of the analysis indicate that the modification mechanism of nano-particles is significantly linked to the trapped electrons process. Specifically, the addition of nano-particles can affect the electrons' density and thus affect the breakdown process and streamer morphology.

Keywords: modification mechanism; pure transformer oil; nano-liquids; streamer morphology; breakdown strength

1. Introduction

Pulsed power technology permits the electric energy to be stored at relatively low power, and be transformed into the electromagnetic energy by pulse and then released into the load to achieve much higher instantaneous power [1]. Pulsed power technology plays an important role in controlled nuclear fusion [2], high-energy accelerator [2], and electromagnetic weapons [3–6]. For example, the pulse generator can generate high instantaneous power and low average power, which may benefit the production of plasma [7,8]. In a relatively high-voltage and high-impedance pulsed power system with the lowest possible voltages in initial energy storage and switching, which can be used to design the electron ring accelerator [2].

The pulsed power system is mainly composed of the primary energy-storage systems, pulse compression systems, and high-power load systems [9–11]. As the key components in primary energy-storage systems, the liquid mediums are often used for energy storage and insulation because of their excellent characteristics such as high-energy storage density, great self-healing effects, and good thermal conductivity [12,13]. The commonest liquid mediums include water medium and oil medium [14,15]. Due to the rapid decreases in water resistivity, the oil medium would be more applicable to a pulse generator. Moreover, the breakdown strength of the oil medium can exceed 300 kV/cm after purification treatment.

However, solid impurities are inevitably introduced when pouring the oil medium into the pulse generator, which substantially affects the insulation performance of transformer oil [16–18]. In practical production, the insulation performance of transformer oil not only affects the operational reliability of pulsed power system, but it also largely determines the cost of oil-insulated electrical equipment [19–21]. Therefore, it is of great significance to ensure the safe operation of the pulsed power system by improving the insulation performance of transformer oil [22–25].

In traditional dielectric theory, impurities in transformer oil gather and recombine into a conductive "bridge" under the applied electric field, which leads to the reduction in insulation performance. However, Segal et al. discovered that the breakdown strength of transformer oil under positive impulse breakdown voltage can be improved by introducing the Fe_3O_4 nano-particles, which contradicted the traditional principle that the insulation performance of liquid mediums is proportional to purity [26]. Researchers have since paid attention to nano-modification technology. With the depth of the research work, many researchers have realized that some parameters such as the type, shape, and surface modification of nano-particles will have a great influence on the modification effect [27–30]. Specifically, the insulation performance of transformer oil can be characterized by the breakdown strength, which is related to the pre-breakdown phenomenon defined as the "streamer" in transformer oil [31–34].

In order to explain the modification effect and streamer morphology in nano-liquid, several breakdown models and mechanisms have been proposed. Hwang et al. established an electrodynamic model for the formation of the streamer in nano-liquids and then proposed the corresponding nano-particles electron-trapping theory [24,25]. Li et al. proposed a shallow trap model associated with the charge-hopping process in nano-liquids, which demonstrated that the improvement in shallow trap density will promote the formation of a uniform internal electric field and reduce the charge accumulation in the streamer head [35,36]. Sima et al. proposed a barrier ionization model that analyzed the effect of nano-particles on the electron capture process and insulation performance [37,38]. Lewis et al. proposed a new model to illustrate the streamers in liquid mediums based on the mechanical stress generated by the electric field [31].

However, for the initiation mechanism of the impact of nano-particles on the modification effect and streamer morphology, no consensus has been reached. In addition, the above models were discussed by a simulating analysis which lacks the necessary experimental evidence. Obviously, analysis of the relationship among nano-particles, streamer morphology, and breakdown strength may provide a valuable insight and experimental evidence to explain the modification effect of nano-liquids. Moreover, it is helpful to provide an improved understanding of the macroscopic breakdown phenomena and microscopic development mechanism.

In this paper, we experimentally investigated the streamer morphology and modification effect in pure transformer oil and nano-liquids. We first set up a platform for microsecond pulse breakdown strength testing and streamer shooting, which is composed of a microsecond pulse generator, breakdown test cell, and high-speed camera. Then, we prepared transformer oil nano-liquids with the addition of Al_2O_3 nano-particles and TiO_2 nano-particles in different volume fractions. In particular, we shot the streamer with a high-speed camera, and measured the breakdown strength under microsecond pulse. By comparing the streamer morphology and modification effect of pure transformer oil and nano-liquids, we found that the addition of nano-particles can significantly affect the streamer morphology and modification effect.

The paper is organized as follows: In Section 2, we briefly introduce the preparation of the nano-liquids, microsecond-pulse breakdown strength test platforms, and explain how a breakdown experiment is performed in this system. In Section 3, by measuring and comparing the streamer morphology and breakdown strength in nano-liquids, we found that the addition of nano-particles significantly affects the streamer morphology and breakdown strengths. In Section 4, we discuss the behavior of nano-particles in liquid mediums to explain the variation in streamer morphology and breakdown strength. Finally, conclusions are drawn in Section 5.

2. Set-Up and Experimental Method

The Karamay 45 transformer oil for national test standard GB/T 507 was chosen as the base liquid, whose breakdown voltage can reach 70 kV after a series of filtration and purification [39]. It has been demonstrated that the semiconductor nano-particles have the potential to improve the insulation performance [40]. In our experiments, we purchased the TiO_2 nano-particles and Al_2O_3 nano-particles with diameters of 30 nm from DKNANO (Beijing, China).

The typical preparation processes of nano-liquids are as follows: First, the nano-particles should be dried in vacuum at 100 °C for 24 h. Then, these nano-particles were dispersed in the transformer oil for about an hour by the use of planetary and vertical mixers. Subsequently, the mixtures were poured into an ultrasonic pulverizer for about 0.5 h. In the end, the mixtures were ground in an agate pot for 24 h. By repeating these processes, we prepared the evenly dispersed TiO_2 nano-liquids and Al_2O_3 nano-liquids with different volume fractions [41].

The experimental equipment is shown in Figure 1 and is composed of a microsecond pulse generator, breakdown test cell, and high-speed frequency camera(HSFC). Specifically, the microsecond pulse generator shown in Figure 1a can output 380 kV peak voltage with 10 µs pulse width for a single microsecond pulse. As shown in Figure 1b, the breakdown test cell is a 20 cm hollow hexahedron based on a standard oil cup. In particular, it comes with a built-in brass needle-plate electrode with an electrode gap of 2 mm when shooting the streamer. There is another case where, when measuring the breakdown voltage, the brass spherical electrodes with an electrode gap of 0.5 mm were inlaid. The high-speed camera, model HSFC-pro, is shown in Figure 1c, which is used for the shooting of streamer. The exposure time of the high-speed camera can be adjusted between 3 and 1000 ns and the grayscale value in the range of 0 to 4096, which can capture photographs with 1280- by 1024-pixel.

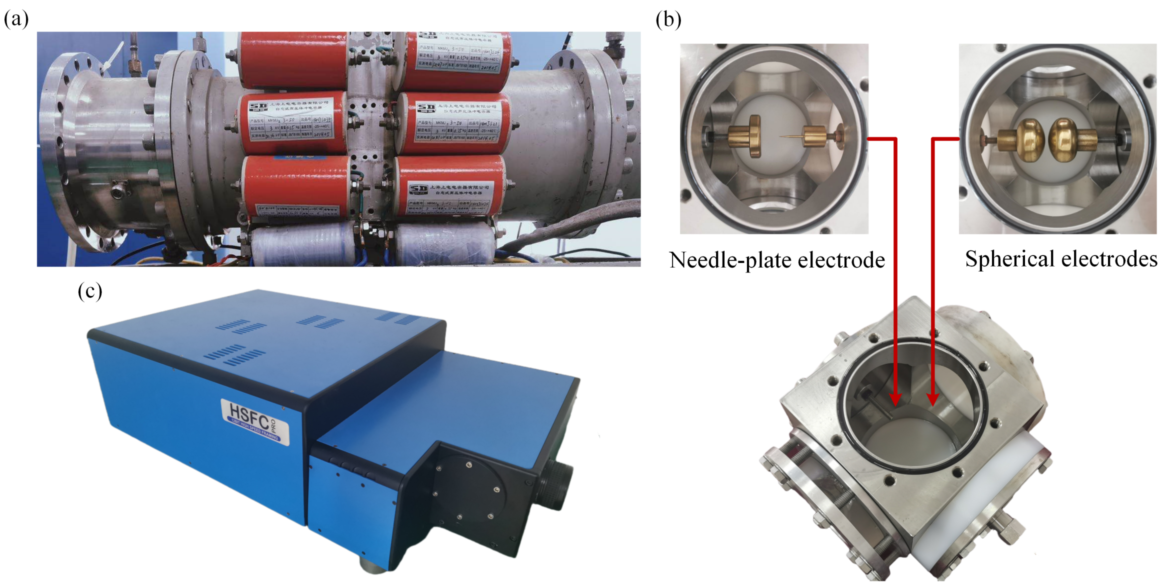

Figure 1. Experimental equipments of the microsecond-pulse breakdown strength test platforms: (**a**) microsecond pulse generator, (**b**) breakdown test cell, and (**c**) HSFC-pro high-speed camera.

The simulation circuit diagram is shown in Figure 2. Under the room temperature (approximately 25 °C) and standard atmospheric pressure (0.1 MPa), the system is powered by the main supply (220 V/50 Hz), and the primary capacitor is adjusted to 200 V by the voltage regulator. The trigger outputs two synchronizing signals: one controls the conduction of the main thyristor, and the other controls the HSFC-pro high-speed camera.

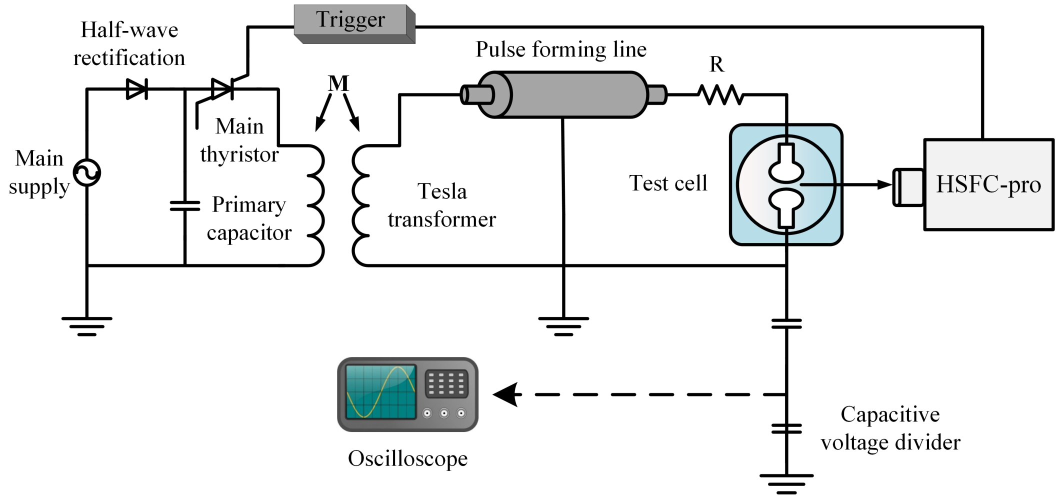

Figure 2. Schematic diagram of the microsecond pulse breakdown strength test platform.

When the circuit is triggered, the primary capacitor is boosted and the pulse-forming line is charged under Tesla transformer. With the increase in pulse voltage, the liquid breaks down when voltage goes beyond the threshold level (breakdown voltage). Once the breakdown occurs, the high-speed camera shoots the streamer at the same time. Since the development time of streamer refers to nanoseconds, we chose the exposure time of 3 ns. Figure 3 shows the breakdown waveforms obtained by the oscilloscope; the typical voltage-rising duration from trough to peak is approximately 10 µs.

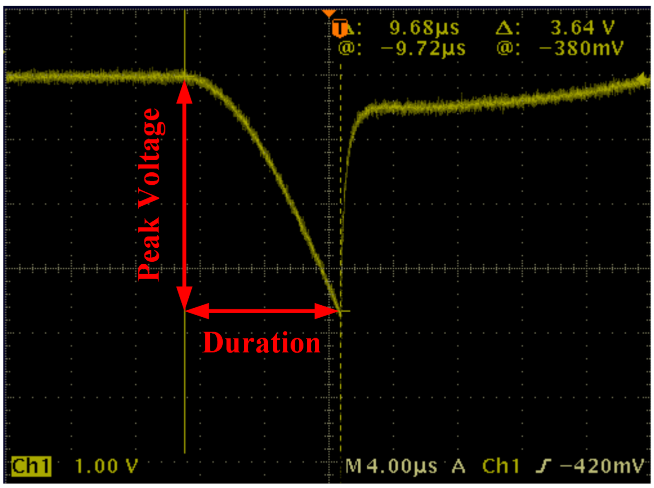

Figure 3. Typical breakdown waveforms obtained by the oscilloscope. The typical voltage-rising duration is approximately 10 µs.

3. Experimental Results and Analysis

3.1. Streamer Analysis

To explore the impact of nano-particles on transformer oil, we measured and compared the streamer morphology of pure transformer oil and nano-liquids. Considering the poor translucency under higher volume fractions, TiO_2 nano-liquids and Al_2O_3 nano-liquids were prepared with volume fraction of 0.002%.

As shown in Figure 4a1–a5, b1–b5, c1–c5 are the streamer morphology of pure transformer oil, TiO_2 nano-liquids, and Al_2O_3 nano-liquids shot by high-speed camera, respectively. Note that each liquid here was tested 20 times and we randomly selected five sets of typical streamers for each liquid.

As we can see, there is a conspicuous difference between the pure transformer oil and nano-liquid in streamer morphology.

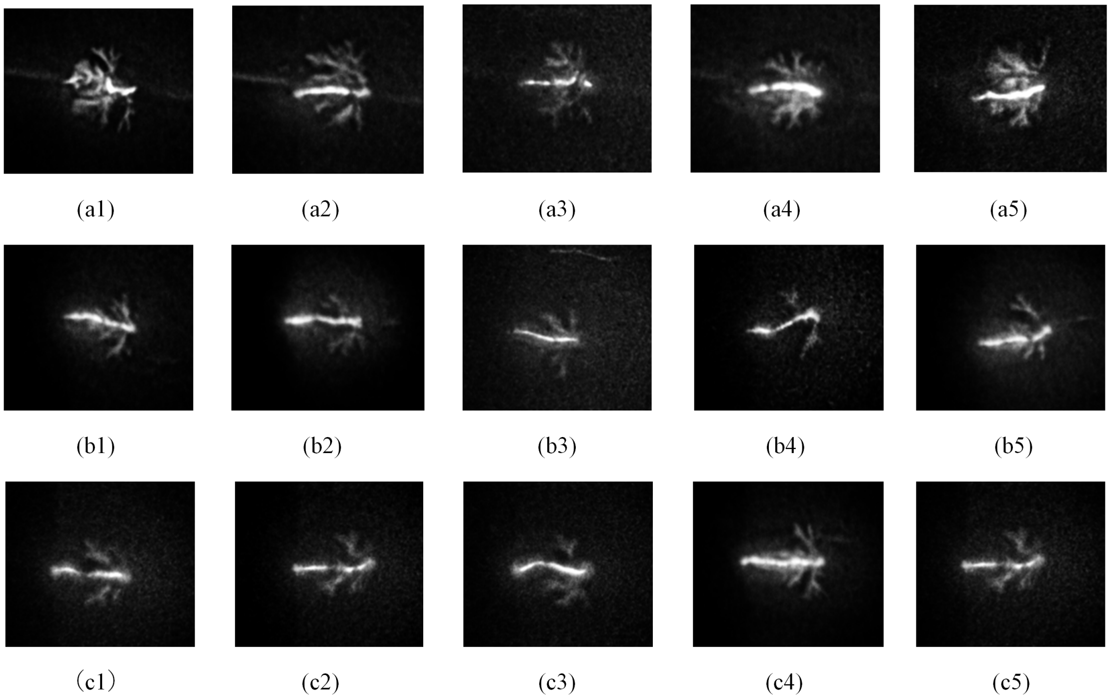

Figure 4. The streamer morphology of pure transformer oil and nano-liquids shot by high-speed camera. (**a1**–**a5**) pure transformer oil, (**b1**–**b5**) TiO_2 nano-liquids, (**c1**–**c5**) Al_2O_3 nano-liquids.

In order to facilitate the analysis and discussion, we plotted the schematic diagram of streamer morphology in Figure 5. To distinguish the branches of the streamer, we defined the bright channel from needle electrode to plate electrode as the main streamer, the branches on main streamer as the primary streamer branch, and the other branches on primary streamer branch as the secondary streamer branch.

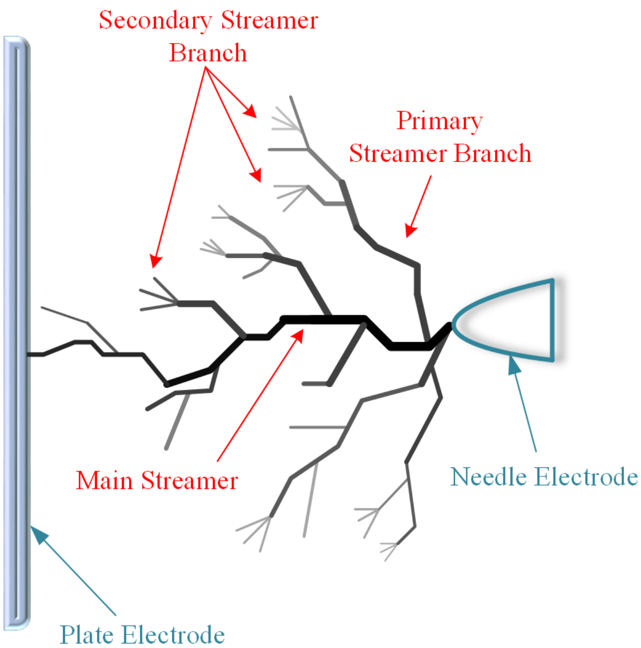

Figure 5. The schematic diagram of streamers.

As we can see in Figure 4a1–a5, the streamers in pure transformer oil exhibit thick bush-like qualities. Certain nodes in the main streamer bifurcate and develop into primary streamer branches, then additional nodes are updated in primary streamer branches with more dispersed secondary streamer branches. While in the case of Figure 4b1–b5,c1–c5, the streamers in TiO_2 nano-liquids and Al_2O_3 nano-liquids exhibit tree-like qualities. The bifurcation nodes are mainly distributed in the head of the main streamer with a few primary streamer branches. Moreover, the propagation length of primary streamer branches is much shorter than that in pure transformer oil, which is accompanied by less secondary streamer branches. In consequence, the overall morphology of streamers in nano-liquids is more sparse than that in pure transformer oil. This suggests that the addition of TiO_2 nano-particles and Al_2O_3 nano-particles significantly affects the streamer morphology.

3.2. Breakdown Characteristics Analysis

As discussed in the previous section, the number of streamer branches decreased significantly in nano-liquids, which are accompanied by fewer and shorter secondary streamer branches. Further research is needed to explore the modification mechanism of nano-particles on transformer oil, therefore, we measured the breakdown voltage of transformer oil, TiO_2 nano-liquids and Al_2O_3 nano-liquids with a series of volume fractions. Based on the analysis of breakdown voltage and combined with the previous empirical research, when the order of magnitudes of the volume fraction nano-liquids reaches 0.1% [42,43], there would be an obvious modification effect, i.e., the increase in the breakdown strength of the liquid dielectric after nano-modification. Considering the modification effect on microsecond pulse, we chose the typical volume fractions ranging from 0.2% to 0.8% [41]. Twenty repeat breakdown strength measurements were applied for each group.

There is a uniform distributed electric field between the two spherical electrodes; the breakdown strength E can be expressed as [42]

$$E = U/d \tag{1}$$

where U is the breakdown voltage, d is the electrode gap. The Weibull distribution has been proved to be appropriate for the estimation of average breakdown field strength associated with the probability of breakdown, and the probability of cumulative percentage of breakdowns is defined by [44,45]

$$P(U) = 1 - e^{-(U/\alpha)^{\beta}} \tag{2}$$

where α is the scale parameter representing the characteristic breakdown voltage, and β is the shape parameter measuring the sensitivity of the insulation system.

Figure 6 shows the Weibull distribution of pure transformer oil, TiO_2 nano-liquids and Al_2O_3 nano-liquids with the volume fractions ranging from 0.2% to 0.8%. When the volume fraction of nano-liquids is 0.2%, there is a clear intersect interference of Weibull distribution between nano-liquids and pure transformer oil, which means a similar average breakdown strength. Furthermore, the average breakdown strength of nano-liquids gradually increases with the volume fractions when the volume fraction is below 0.6%, and then it is started to fall when the volume fraction is beyond 0.6%, which indicates that 0.6% is the threshold level for positive influence and represents the optimal volume fraction of the two nano-liquids.

Table 1 compared the average breakdown strength and modification effect of the pure transformer oil and nano-liquids. The modification effect of TiO_2 nano-liquids ranged from 2.3 to 18% and the modification effect of Al_2O_3 nano-liquids ranged from 5 to 18%. The results have further proven that 0.6% is the optimal volume fraction for the two types of nano-liquid. In general, it is indicated that there is a deep connection between the breakdown strength and nano-particles.

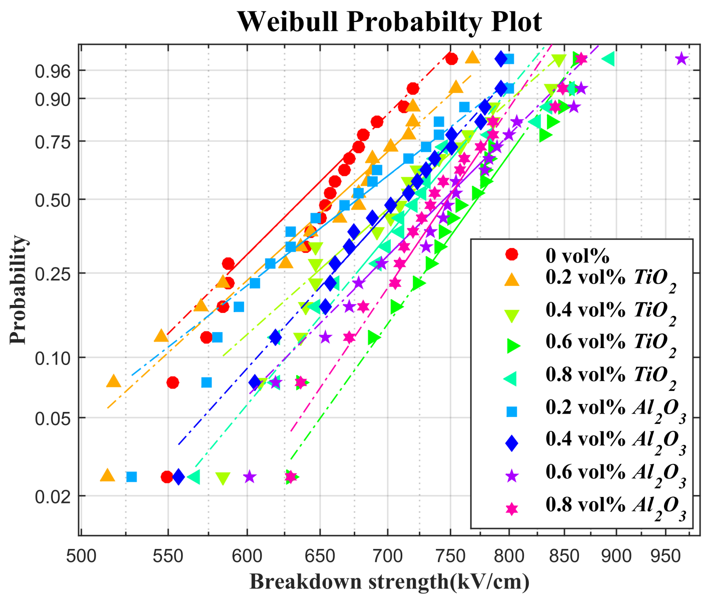

Figure 6. Weibull distribution of pure transformer oil and nano-liquids' breakdown strength with volume fractions of added TiO_2 nano-particles and Al_2O_3 nano-particles ranged from 0.2% to 0.8%.

Table 1. The average breakdown strength and modification effect of TiO_2 and Al_2O_3 nano-liquids. BS represents the average breakdown strength, which is expressed in units of (kV/cm), and ME represents the modification effect.

Volume Fractions	BS_{TiO_2}(kV/cm)	$BS_{Al_2O_3}$ (kV/cm)	ME_{TiO_2}	$ME_{Al_2O_3}$
0%	670.6	670.6	0%	0%
0.2%	686.2	704.6	2%	5%
0.4%	741.9	729.9	11%	9%
0.6%	791.5	790.3	18%	18%
0.8%	761.7	770.7	14%	15%

In order to explore how nano-particles affect the modification effect, optimal volume fraction, and streamer morphology, we discuss the electric field distribution (potential barrier) and hydromechanical properties around TiO_2 nano-particles and Al_2O_3 nano-particles in the next section of this article.

4. Discussion

To further investigate the modification mechanism of nano-particles, we discuss the behavior of nano-particles in liquid mediums. To date, the polarization of nano-particles has been fully proved under the applied electric field. The charges will distort the electric field and accumulate on the surface of nano-particles, which form a "barrier" around the nano-particles [37,38]. Due to the mobility of electrons largely outweighing the ions, our primary concern here is the movement of electrons. While nano-particles can capture electrons and reassemble into negatively charged nano-particles, the breakdown process is suppressed, which can explain why the breakdown strength of nano-liquids is improved after nano-modification in our experiment.

The modification effect is closely associated with the trapped electrons process by the polarized nano-particles, which in turn, is significantly affected by the interface between nano-particles and base liquids. Researchers have found a positive correlation between the modification effect and interface, which is greatly affected by the volume fractions [43,46]. Consequently, we discuss the interface between nano-particles and base liquids in different volume fractions.

As a special colloid, the stability of nano-liquids can be improved by lowering the potential energy of nano-particles. According to the DLVO (Derjaguin, Landau, Verwey and Overbeek) theory, we can obtain the attractive potential energy V_A and repulsive potential energy V_R by analyzing the van der Waals force and electric double-layer forces [47,48]

$$V_A = -\frac{H}{12}\left(\frac{1}{x^2+2x} + \frac{1}{x^2+2x+1} + 2ln\frac{x^2+2x}{x^2+2x+1}\right) \tag{3}$$

$$V_R = \frac{64\pi rcST\gamma^2}{k^2}e^{-ka} \tag{4}$$

where $x = \frac{a-2r}{2r}$, $\gamma = \frac{zq\varphi_0}{4ST}$, $k = (\frac{N_A cz^2 q^2}{\varepsilon ST})^{\frac{1}{2}}$, H is the Hamaker constant, r is the particle radius, a is the centroid distance, T is the temperature of nano-liquids, z is the charge number in base liquids, q is the unit charge, φ_0 is the surface potential of nano-particles, ε is the dielectric constant of base liquids, and others are the constant related to the liquid state. The potential energy V of nano-particles is equal to the sum of the attractive and repulsive potential energy

$$V = V_A + V_R \tag{5}$$

The potential energy V of nano-particles is related to many factors, such as particle radius, centroid distance and temperature. The stability of nano-liquids is directly affected by potential energy. The lower the potential energy, the more stable the system. Because of the small particle size (about 1–100 nm), there is a high surface energy and specific surface area in nano-particles. In order to analyze the interaction forces between the suspended nano-particles, we assumed that the nano-particles are spherical particles of the same size and evenly dispersed. The attractive force F_A and repulsive force F_R between nano-particles can be obtained by

$$F_A = -\frac{dV_A}{dL} = -\frac{dV_A}{dx}\frac{dx}{dL} = \frac{H}{6ax^2(x+2)^2(x+1)^3} \tag{6}$$

$$F_R = -\frac{dV_R}{da} = -\frac{1}{2}\varepsilon rk\varphi_0^2 e^{-ka} \tag{7}$$

From the perspective of thermodynamics, the polymerization of nano-particles under constant temperature and constant pressure is a fully spontaneous process, while the essential purpose is to reduce the surface free energy in nano-particle suspension and tending to stability. Furthermore, the clustered aggregates with big size and mass have a tendency of precipitation under the influence of gravity.

Based on the above analysis, the quantity of added particles increases with the increase in volume fractions, which improves the interface between nano-particles and base liquids and results in a positive influence on the modification effect. However, with the increase in the volume fractions, the centroid distance between nano-particles decreases, which increased the attractive force F_A of nano-particles, thus the nano-particles with smaller size accelerated the tendency of polymerizing into larger size particles. Some larger size particles tend to precipitate, which will reduce the interface between nano-particles and base liquids, thus resulting in a negative influence on the modification effect.

With the increasing process of volume fraction, the negative influence and positive influence restrict and promote each other. When volume fraction is smaller than the threshold level, the positive effect is significantly greater than the negative effect and the modification effect increases with the volume fraction. On the contrary, the negative effect is significantly greater than the positive effect and the modification effect decreases with volume fraction when the volume fraction is higher than the threshold level. In consequence, there would be an optimal volume fraction, which is consistent with the experimental results of Figure 6.

Nano-particles not only affects the breakdown process, but it can also affect the morphology of streamer. With the constant accumulation of electrons in certain nodes of streamer, the interface stability between nodes and base liquids would reduce [49,50]. When the electron density in certain nodes of main streamer reaches a threshold level, the electrons will diffuse and then bifurcate into primary streamer branches [51]. Similarly, when the electron density in certain nodes of primary streamer branches reaches a threshold level, the electrons will diffuse and then bifurcate into secondary streamer branches. Based on the charge conservation theorem, with the increase in primary streamer branches and secondary streamer branches, the electron density in the nodes will decrease. As a consequence, the streamer branches cannot continue to develop into bifurcation when the electrons are less than the threshold level.

As shown in Figure 7a, there are abundant electrons in pure transformer oil, which promote the formation of streamer branches. With the continuous development of the streamer branches, the electron density gradually decreases until the normal bifurcation process is completed. Therefore, the streamers in pure transformer oil with exuberant streamer branches and longer propagation distance, which is consistent with the thick bush-like results in Figure 4a1–a5. However, in the nano-liquids in Figure 7b, the nano-particles will capture the electrons and then reassemble into negatively charged nano-particles, which would result in a lower electron density and streamer branches. As electrons have been captured by nano-particles before the development process of the streamer, the electrons for further bifurcation are drastically reduced. Therefore, the number of streamer branches significantly decreases after nano-modification. This explains why streamers in nano-liquids exhibit tree-like qualities with sparse streamer branches and shorter propagation distances, as shown in Figure 4b1–b5,c1–c5.

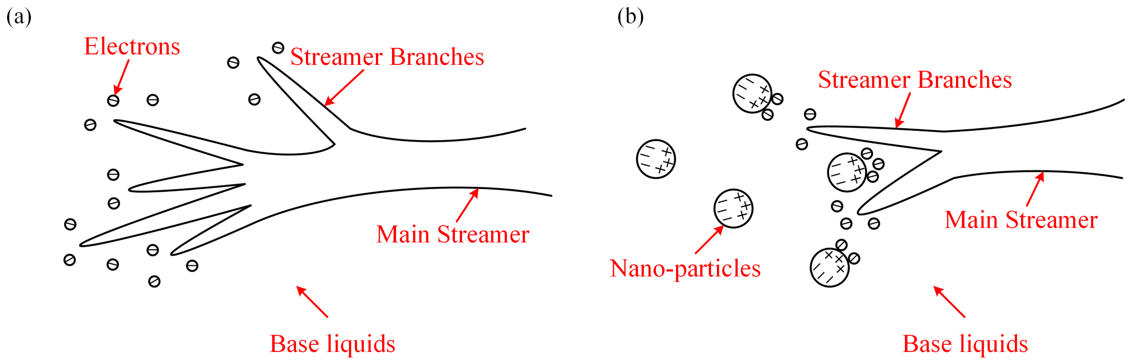

Figure 7. The process of nano-particles trapped electrons in pure transformer oil and nano-liquids. (**a**) Pure transformer oil; (**b**) Nano-liquids.

5. Conclusions

In this study, to explore the modification mechanism of nano-liquids, we measured the streamer morphology and breakdown strength in pure transformer oil, TiO_2 nano-liquids and Al_2O_3 nano-liquids. Based on the results, the following main conclusions are drawn as follows:

1. The streamers in pure transformer oil exhibit thick bush-like qualities with many dispersed streamer branches, while in nano-liquids exhibit tree-like qualities with less sparse streamer branches;
2. The addition of nano-particles can enhance the breakdown strength of transformer oil. With the increase in the volume fractions in nano-liquids, the negative influence on the modification effcet would counterbalance the positive influence on modification effect, and there would be a optimal volume fraction when maintaining a state of equilibrium between negative influence and positive influence.

In conclusion, the modification mechanism of nano-liquids is significantly linked with the trapped electrons process by polarized nano-particles. Specifically, the electron density is an important parameter that affects the streamer morphology and breakdown process. On the one hand, the greater the electron density in certain nodes of streamer, the more and more dispersed the streamer branches.

On the other hand, the greater the electron density in liquid mediums, the easier the breakdown process. While nano-particles can capture electrons and reassemble into negatively charged nano-particles, first of all, this will result in the reduction of electron density in certain nodes of streamer and then result in the reduction of streamer branches; secondly, it will result in the reduction in electron density in liquid mediums and then result in the inhibition of the breakdown process, which means that a higher breakdown voltage is required for the breakdown process.

Author Contributions: Conceptualization, D.L., Z.Z.; methodology, D.L.; experiment, D.L.; validation, Z.Z.; writing—original draft preparation, D.L.; writing—review and editing, D.L. and S.L. (Shifei Liu); supervision, S.L. (Shifei Liu) and S.L. (Song Li). All authors have read and agreed to the published version of the manuscript.

Funding: This research received external funding of the National Natural Science Foundation of China (Grant No. 51677190) and the Hunan Outstanding Youth Fund Project (Grant No. 2017JJ1005).

Acknowledgments: We thank the National Natural Science Foundation of China (Grant No. 51677190) and the Hunan Outstanding Youth Fund Project (Grant No. 2017JJ1005) for supporting this research.

Conflicts of Interest: The authors declare no conflict of interest.

References

1. Zhang, Z.-C.; Zhang, J.-D.; Qian, B.-L.; Liu, C.B.; Xun, T.; Zhang, H.; Liang, B. Compact rep-rate GW pulsed generator based on forming line with built-in high-coupling transformer. *IEEE Trans. Plasma Sci.* **2014**, *42*, 241–248. [CrossRef]
2. Levine, L.S.; Vitkovitsky, I.M. Pulsed power technology for controlled thermonuclear fusion. *IEEE Trans. Nucl. Sci.* **1971**, *18*, 255–264. [CrossRef]
3. McNab, I.R. Developments in pulsed power technology. *IEEE Trans. Magn.* **2001**, *37*, 375–378. [CrossRef]
4. Del Guercio, M. A 4.5-MJ pulsed power supply for railgun experiments. *IEEE Trans. Magn.* **2003**, *39*, 280–284. [CrossRef]
5. Jin, Y.S.; Kim, Y.B.; Kim, J.S.; Cho, C.; Yang, K.S.; Kim, S.H.; Koo, I.S. A 4.8-MJ pulsed-power system for electromagnetic launcher experiment. *IEEE Trans. Plasma Sci.* **2015**, *43*, 3369–3373. [CrossRef]
6. Le, D.V.; Go, B.S.; Song, M.G.; Park, M.; Yu, I.K. Development of a capacitor bank-based pulsed power supply module for electromagnetic induction coilguns. *IEEE Trans. Plasma Sci.* **2019**, *47*, 2458–2463. [CrossRef]
7. Dong, S.; Yao, C.; Yang, N.; Luo, T.; Zhou, Y.; Wang, C. Solid-state nanosecond-pulse plasma jet apparatus based on Marx structure with crowbar switches. *IEEE Trans. Plasma Sci.* **2016**, *44*, 3353–3360. [CrossRef]
8. Rao, J.; Lei, Y.; Jiang, S.; Li, Z.; Kolb, J.F. All solid-state rectangular sub-microsecond pulse generator for water treatment application. *IEEE Trans. Plasma Sci.* **2018**, *46*, 3359–3363. [CrossRef]
9. Martin, J.C. Nanosecond pulse techniques. *Proc. IEEE* **1996**, *80*, 934–945. [CrossRef]
10. Schamiloglu, E.; Barker, R.J.; Gundersen, M.; Neuber, A.A. Modern Pulsed Power: Charlie Martin and Beyond. *Proc. IEEE* **2004**, *92*, 1014–1020. [CrossRef]
11. Li, S.; Gao, J.-M.; Shi, C.-Y.; Liu, X.; Yang H.-W. Investigation on a fast rise time high voltage pulse transformer. *Rev. Sci. Instrum.* **2019**, *90*, 124707. [CrossRef] [PubMed]
12. Pislaru-Danescu, L.; Morega, A.M.; Telipan, G.; Morega, M. Magnetic Nanofluid Applications in Electrical Engineering. *IEEE Trans. Magn.* **2013**, *49*, 5489–5497. [CrossRef]
13. Sartoratto, P.P.C.; Neto, A.V.S.; Lima, E.C.D.; Rodrigues De Sa, A.L.C.; Morais, P.C. Preparation and electrical properties of oil-based magnetic fluids. *J. Appl. Phys.* **2005**, *97*, 10Q917. [CrossRef]
14. Zahn, M.; Ohki, Y.; Fenneman, D.B. Dielectric properties of water and water/ethylene glycol mixtures for use in pulsed power system design. *Proc. IEEE* **1986**, *74*, 1182–1221. [CrossRef]
15. Jin, H.-F.; Andritsch, T.; Tsekmes, I.A.; Kochetov, R.; Morshuis, P.H.F.; Smit, J.J. Properties of mineral oil based silica nanofluids. *IEEE Trans. Dielectr. Electr. Insul.* **2014**, *21*, 1100–1108.
16. Joshi, R.P.; Thagard, S.M. Streamer-Like Electrical Discharges in Water: Part I. Fundamental Mechanisms. *Plasma Chem. Plasma Process.* **2013**, *33*, 1–15. [CrossRef]
17. Joshi, R.P.; Kolb, J.F.; Xiao, S.; Schoenbach, K.H. Aspects of Plasma in Water: Streamer Physics and Applications. *Plasma Process. Polym.* **2009**, *6*, 763–777. [CrossRef]

18. Stygar, W.A.; Savage, M.E.; Wagoner, T.C.; Bennett, L.F.; Corley, J.P.; Donovan, G.L.; Fehl, D.L.; Ives, H.C.; LeChien, K.R.; Leifeste, G.T.; et al. Dielectric-breakdown tests of water at 6MV. *Phys. Rev. Accel. Beams* **2009**, *12*, 308–312.
19. Okabe, S. Evaluation of breakdown characteristics of oil-immersed transformers under non-standard lightning impulse insulation characteristics for non-standard lightning impulse waveforms with oscillations. *IEEE Trans. Dielectr. Electr. Insul.* **2007**, *14*, 679–688. [CrossRef]
20. Okabe, S.; Takami, J. Evaluation of breakdown characteristics of oil-immersed transformers under non-standard lightning impulse waveforms-method for converting non-standard lightning impulse waveforms into standard lightning impulse waveforms. *IEEE Trans. Dielectr. Electr. Insul.* **2008**, *15*, 1288–1296. [CrossRef]
21. Wedin, P. Electrical breakdown in dielectric liquids—A short overview. *IEEE Electr. Insul. Mag.* **2014**, *30*, 20–25. [CrossRef]
22. Pezeshkim H., Wolfsm P.J., Ledwich, G. Impact of High PV Penetration on Distribution Transformer Insulation Life. *IEEE Trans. Power Deliv.* **2014**, *29*, 1212–1220. [CrossRef]
23. Liang, J.; Zhang, L.; Li, J.; Li, Y. Study on Oscillating Switching Impulse Voltage Generation for Power Transformer Onsite Test. *IEEE Trans. Power Deliv.* **2014**, *29*, 2223–2230. [CrossRef]
24. Hwang, J.G.; O'Sullivan, F.; Zahn, M.; Hjortstam, O.; Liu, R.S. Modeling of Streamer Propagation in Transformer Oil-Based Nanofluids. In Proceedings of the 2008 Annual Report Conference on Electrical Insulation and Dielectric Phenomena, Quebec, QC, Canada, 26–29 October 2008; pp. 361–366.
25. Hwang, J.G.; Zahn, M.; O'Sullivan, F.M.; Pettersson, L.A.A.; Hjortstam, O.; Liu, R.S. Effects of nanoparticle charging on streamer development in transformer oil-based nanofluids. *J. Appl. Phys.* **2010**, *107*, 416–622. [CrossRef]
26. Segal, V.; Hjortsberg, A.; Rabinovich, A.; Nattrass, D.; Raj, K. AC (60 Hz) and impulse breakdown strength of a colloidal fluid based on transformer oil and magnetite nanoparticles. *Chem. Phys. Lett.* **2016**, *662*, 192–195.
27. Nadolny, Z.; Dombek, G. Electro-Insulating Nanofluids Based on Synthetic Ester and TiO_2 or C60 Nanoparticles in Power Transformer. *Energies* **2018**, *11*, 1953. [CrossRef]
28. Lue, Y.-F.; Hung, Y.-H.; Li, F.-S.; Teng, T.-P.; Chen, S.-Y.; Wu, C.-H.; Ou, Y.-C. Performance Assessment and Scooter Verification of Nano-Alumina Engine Oil. *Appl. Sci.* **2016**, *6*, 258. [CrossRef]
29. Li, J.; Du, B.; Wang, F.; Yao, W.; Yao, S. The effect of nanoparticle surfactant polarization on trapping depth of vegetable insulating oil-based nanofluids. *Phys. Lett. A* **2015**, *380*, 604–608. [CrossRef]
30. Abhishek, R.; Hamouda, A.A. Effect of Various Silica Nanofluids: Reduction of Fines Migrations and Surface Modification of Berea Sandstone. *Appl. Sci.* **2017**, *7*, 1216. [CrossRef]
31. Lewis, T.J. A new model for the primary process of electrical breakdown in liquids. *IEEE Trans. Dielectr. Electr. Insul.* **1998**, *5*, 306–315. [CrossRef]
32. Korobeynikov, S.M.; Melekhov, A.V. Nonelectrode Streamers in Deionized Water. *IEEE Trans. Plasma Sci.* **2011**, *39*, 2632–2633. [CrossRef]
33. Korobeynikov, S.M.; Melekhov, A.V.; Posukh, V.G.; Ponomarenko, A.G.; Boyarintsev, E.L.; Antonov, V.M. Optical study of prebreakdown cathode processes in deionized water. *IEEE Trans. Dielectr. Electr. Insul.* **2009**, *16*, 504–508. [CrossRef]
34. Linhjell, D.; Lundgaard, L.; Berg, G. Streamer propagation under impulse voltage in long point-plane oil gaps. *IEEE Trans. Dielectr. Electr. Insul.* **1994**, *1*, 447–458. [CrossRef]
35. Du, Y.; Lv, Y.; Li, C.; Chen, M.; Zhong, Y.; Zhang, S.; Zhou, Y. Effect of nanoparticles on charge transport in nanofluid-impregnated pressboard. *J. Appl. Phys.* **2012**, *111*, 124322. [CrossRef]
36. Ge, Y.; Lv, Y.Z.; Han, Q.B.; Sun, Q.; Yuan, J.S. Effects of TiO2 Nanoparticles on Streamer Propagation at the Surface of Oil-Impregnated Insulation Paper. *IEEE Trans. Plasma Sci.* **2018**, *99*, 1–6. [CrossRef]
37. Sima, W.-X.; Cao X.-F.; Yang, Q.; Song, H.; Shi, J. Preparation of Three Transformer Oil-Based Nanofluids and Comparison of Their Impulse Breakdown Characteristics. *Nanosci. Nanotechnol. Lett.* **2014**, *6*, 250–256. [CrossRef]
38. Shi, J.; Yang, Q.; Sima, W.X.; Yu, F. Surface Modification of Nanoparticle and Its Charging Dynamics During Streamer Discharge in Transformer Oil. *Nanosci. Nanotechnol. Lett.* **2014**, *6*, 424–430.
39. Gao, M.; Li G.-F.; Li, J.-Z.; Zhao, Z.-G. The temperature dependence of insulation characteristics of transformer oil at low temperatures. In Proceedings of the IEEE Power Engineering and Automation Conference, Wuhan, China, 8–9 September 2011; Volume 2; pp. 27–30.

40. Hou, Y.-P.; Zhang, Z.-C.; Zhang, J.-D. Significantly Enhanced Impulse Breakdown Performances of Propylene Carbonate Modified by TiO_2 Nano-particles. *Chem. Phys. Lett.* **2016**, *662*, 192–195. [CrossRef]
41. Hou, Y.-P.; Zhang, Z.-C.; Zhang, J.-D.; Liu, Z.-F.; Song, Z.-Y. Effect of $BaTiO_3$ nano-particles on breakdown performance of propylene carbonate. *Rev. Sci. Instrum.* **2015**, *86*, 241–248. [CrossRef]
42. Hou, Y.-P.; Zhang, Z.-C.; Zhang, J.-D.; Wang, Z.; Liu, H.-W. Experimental investigations into the enhanced dielectric breakdown performances of propylene carbonate modified by TiO_2 nano-particles. *IEEE Trans. Dielectr. Electr. Insul.* **2016**, *23*, 2816–2821. [CrossRef]
43. Hou, Y.-P.; Zhang, J.-D.; Zhang, Z.C.; Wang, Z.; Song, Z.-Y. Experimental study on breakdown characteristics of propylene carbonate-based nano-fluids under microsecond pulses. In Proceedings of the IEEE Pulsed Power Conference, Austin, TX, USA, 31 May–4 June 2015; Volume 133, pp. 1–5.
44. Laurent, C.; Chauvet, C. The significance of the Weibull threshold in short-term breakdown statistics. *IEEE Trans. Dielectr. Electr. Insul.* **1994**, *1*, 160–162. [CrossRef]
45. Wilson, M.P.; Given, M.J.; Timoshkin, I.V.; MacGregor, S.J.; Wang, T.; Sinclair, M.A.; Thomas, K.J.; Lehr, J.M. Impulse-driven surface breakdown data: A weibull statistical analysis. *IEEE Trans. Plasma Sci.* **2012**, *40*, 2449–2456. [CrossRef]
46. Hashemi, R.; Nassar, N.N.; Almao, P.P. Nanoparticle technology for heavy oil in-situ upgrading and recovery enhancement: Opportunities and challenges. *IEEE Trans. Dielectr. Electr. Insul.* **2014**, *133*, 374–387. [CrossRef]
47. Qian, J.; Joshi, R.P.; Schamiloglu, E.; Gaudet, J.; Woodworth, J.R.; Lehr, J. Analysis of polarity effects in the electrical breakdown of liquids. *IEEE Trans. Plasma Sci.* **2006**, *39*, 359. [CrossRef]
48. Adamczyk, Z.; Weronski, P. Application of the DLVO theory for particle deposition problems. *Adv. Colloid. Interfac.* **1999**, *83*, 137–226. [CrossRef]
49. Jadidian, J.; Zahn, M.; Lavesson, N.; Widlund, O.; Borg, K. Stochastic and deterministic causes of streamer branching in liquid dielectrics. *J. Appl. Phys.* **2013**, *114*, 6–17. [CrossRef]
50. Luque, A.; Ebert, U. Electron density fluctuations accelerate the branching of positive streamer discharges in air. *Phys. Rev. E* **2011**, *84*, 046411. [CrossRef]
51. Vega, F.; Pérez, A.T. Corona-induced electrohydrodynamic instabilities in low conducting liquids. *Exp. Fluids* **2003**, *34*, 726–735. [CrossRef]